Waste Management 195 (2025) 10–21

Contents lists available at ScienceDirect

Waste Management

journal homepage: www.elsevier.com/locate/wasman

Research Paper

Steam washing for MSWI-FA treatment

Davide Bernasconi [a,*], Caterina Caviglia [a], Enrico Destefanis [a], Costanza Bonadiman [b], Valentina Brombin [b], Maura Mancinelli [b], Renzo Tassinari [b], Alessandro Pavese [a]

[a] Earth Sciences Department, University of Turin 10125 Turin, Italy
[b] Earth Science and Physics Department 44122 Ferrara, Italy

ARTICLE INFO

Keywords:
MSWI-FA
Steam washing
Speciation distribution
Pollutants leaching

ABSTRACT

This study investigates steam washing (SW) as an innovative pretreatment for municipal solid waste incineration fly ash (MSWI-FA) dechlorination, useful for a more effective stabilization in cementitious matrix. By using a detailed analytical approach (XRPD, XRF, ICP-MS, IRMS, SEM) and geochemical modeling, great focus is dedicated on pollutant leaching reduction and changes in ash physicochemical characteristics as a function of exposure time. The research demonstrates that SW removes up to 70 % cadmium, 17 % zinc, and 10 % lead, primarily by dissolving the soluble and carbonate/hydroxide fractions and promoting the reprecipitation and adsorption of heavy metals into more stable compounds. Chloride, sulfate, and heavy metal leaching are reduced by 85 %, 50 %, and 90 %, respectively, with even short treatment time (8 min) performing better than conventional water washing at a liquid-to-solid ratio of 2. However, antimony leaching remains above regulatory thresholds, controlled by soluble Ca-antimonate phases, thus requiring supplementary tailored treatments. Further optimization of the energy recovery during the exposure and a comprehensive life-cycle assessments to evaluate its long-term environmental and economic impact, may contribute significantly to propose SW as a sustainable strategy for MSWI-FA treatment and valorization.

1. Introduction

In Europe, 505 kg per capita of municipal solid waste was generated in 2020 (Eurostat, 2021) and 135 kg per capita were incinerated. Fly ash (FA) from Municipal Solid Waste Incineration (hereafter: MSWI-FA) is estimated to account for approximately 3–10 % of MSW (Kanhar et al., 2020). MSWI-FA is classified as hazardous waste, encoded by the European Commission with the European Waste Code 19 01 13* (European Commission, 2000), because of the content of heavy metals (Zn, Pb, Cu, Cr, Cd and Ni), soluble salts (chloride and sulfate) and the related risk of leaching (Righi et al., 2022). MSWI-FA is expected to increase up to 140 % in 2050 (Watari et al., 2021); in this light, its re-use/recycling would remarkably boost the efficiency of European circular economy strategy.

Although making MSWI-FA an inert waste *via* an environmentally sustainable treatment is still a challenge, the reduction of alkali chlorides (in particular KCl and NaCl) and heavy metals leaching provides a crucial goal to design a potential re-use of fly ash (Xu et al., 2019), for instance in geopolymers or cements (Bernasconi et al., 2023a,b; Aubert et al., 2006; Liu et al., 2022). The leaching behaviors of heavy metals is the result of a complex interplay between how they are bound to the matrix, i.e., their "speciation", and the external conditions, i.e., pH, temperature, and redox potential. Most heavy metals (Zn, Pb, Ni) usually occur as oxides, hydroxides, and carbonates, which are stable at pH around 9–11, but can readily dissolve at acidic pH (Chen et al, 2023). At higher pH values (> 11–12), the dissolution of these heavy metals increases due to the relative stability of their hydroxide complexes in solution, thus displaying an amphoteric behavior (Zhang et al, 2008). Moreover, other heavy metals may display different pH-dependent leaching profiles, even correlated to their oxidation state that affects solubility, i.e., Cr (Cr^{3+} and CrO_4^{2-}) and Sb (Sb^{3+} and $Sb(OH)_6^-$) (Meima et al, 1998).

In addition, competitive adsorption processes with both inorganic reactive surfaces, i.e., Fe/Al oxyhydroxides, and organic fraction (humic acid) can in turn limit and control the heavy metals release, based on the relative strength of their interactions (Dijkstra et al, 2006; Hiemstra et al., 2006). Moreover, the organic matter can comprise toxic and persistent dioxins/furans compounds, which further complicate the design of the treatment strategies (Li et al, 2023).

Water-washing, which is a common method for pre-treating MSWI-FA to remove chloride (Chen et al. 2016), has been the object of many

* Corresponding author.
E-mail address: davide.bernasconi@unito.it (D. Bernasconi).

https://doi.org/10.1016/j.wasman.2025.01.031
Received 6 September 2024; Received in revised form 29 November 2024; Accepted 22 January 2025
Available online 28 January 2025

studies to investigate the role of operational parameters such as liquid-to-solid mass ratio (LS), washing duration and frequency (Ferraro et al. 2019, for a review). Other methods to treat MSWI-FA involve, for instance, vitrification by heating over 900 °C (Nowak et al., 2010); microwave hydrothermal treatments, for an efficient dechlorination and detoxification of POPs (Xue et al., 2021); bioleaching, for heavy metals recovering (Funari et al. 2023).

Acidic leaching is an efficient technique to dissolve phases bearing metals (Hu et al. 2015), and a water extraction process at a L/S $\geq$ 2 allows the removal of more than 95 % of chloride and up to 30 % of sulfate. Multi-step washing is found to be effective, especially in chloride removal, but it requires high volumes of water (Colangelo et al., 2015; Caviglia et al., 2022). In general, conventional water washing implies an extensive consumption of liquid, giving rise to large volumes of wastewater, which, in turn, poses a serious problem in managing the risk of a secondary environmental pollution (Loginova et al., 2019). For this reason, efforts are devoted to developing strategies thatmay provide solutions to reduce the degree of hazardousness of MSWI-FA, while limiting wastewater production.

In this context, Destefanis et al. (2020) introduced the technique of "*steam washing*" (SW), by simulating a typical incineration steam flow and directing it to treat coarse MSWI bottom ash (grain size > 1 mm) through a rapid washing. The SW was developed to exploit a commodity intrinsically available at the WtE plants, thus favoring a possible direct implementation in the process flow and limiting the transportation cost for MSWI ash treatment. All of this had the objective of making the costs of disposal more independent of market fluctuations (Cialani et al., 2020; Mazzanti et al., 2008). In particular, the steam was observed to induce a mechanical removal and mild dissolution of the finer particles on the surface of the BA grains, thus improving the leaching performance of the coarse fraction coupled with a reduction of wastewater volume with respect to a traditional water washing (Destefanis et al., 2020).

The present study was designed to extend the SW to MSWI-FA and investigate its efficiency in terms of curbing heavy metal and chloride/sulfate leaching, in order to promote a conversion towards non-hazardous waste (potentially suitable to solidification/stabilization in cement matrix). An in-depth analytical investigation of both solid and liquid phases by X-Ray Powder Diffraction (XRPD), X-Ray Fluorescence Spectrometry (XRF), Inductively Coupled Plasma-Mass Spectrometry (ICP/MS), Isotope Ratio Mass Spectrometry (IRMS) and Ionic Chromatography (IC) allowed to quantitatively evaluate the treatment performance. Moreover, a sequential extraction procedure coupled with a geochemical modelling approach provided further insight into the process phenomenology.

Although previous works have employed superheated steam in combination with high-temperature treatment (T > 500 °C) (Zhao et al, 2020), to our knowledge, no previous study about the direct application of steam washing treatment to MSWI-FA has been reported in literature.

2. Materials and methods

2.1. Materials

For this study, MSWI-FA from a third-generation (i.e., in operation since after 2006) municipal solid waste incineration plant in northern Italy were used The plant flue gas cleaning system employs a 4-steps process: i) electrofilter after the boiler section; ii) dry scrubber with $NaHCO_3$ and activated carbon (NEUTREC® technology), followed by iii) baghouse filter; iv) ammonia-based catalytic process for NOx reduction.

In particular, about 3 kg of MSWI-FA samples were collected from a homogenized 100 kg batch of a mixture between boiler ash (BOA) and electrostatic precipitator fly ash (ESPA), which are not differentiated in the plant (Wolffers et al., 2021). The MSWI-FA were dried in an oven at 105 °C for 24 h to remove humidity; ten subsamples of 100 g were prepared and analyzed in terms of particle size distribution, with D50 ~ 149 μm (Fig. S1).

2.2. Organization of the work

The work was in: i) raw MSWI-FA full characterization (phase/bulk chemical composition; speciation distribution; chloride/sulfate/heavy metal leaching); ii) analysis of the effect induced by conventional water washing at L/S = 2, in terms of residual leaching from the treated MSWI-FA; iii) analysis of the effect induced by SW, as a function of the exposure time, on the resulting treated MSWI-FA; iv) interpretation of the phenomenology related to SW.

2.3. Steam washing apparatus

The experimental apparatus for SW is a prototype designed and assembled by ETG s.r.l. (Environmental Technology Group), and it is sketched in Fig. 1. It is composed of a steam generator, which uses deionized water. A panel of sensors, to which the steam generator is connected, sets and records the parameters of air flux (L/min), temperature (T°C) and relative humidity (% v/v). A feedback system tunes the steam production as a function of the control parameters. A pipe drives the steam onto MSWI-FA sample, spread on a Buchner funnel with a paper filter that hosts around 10 g of MSWI-FA. A flask is located underneath the sample-holder, with a vacuum pump (P_{max} = -1 bar), to rapidly remove and collect the condensation water from the surface of the MSWI-FA during washing.

The experiments were carried out at a relative humidity (RH) of ~ 40 % v/v, employing a 2 L/min flux, and T = 90 °C (representing a dew-point of 67 °C). Since the operational temperature of the steam at plants is around 120 °C, the lower temperature conditions would allow one the partial recover of energy from the steam before being used in the washing process.

Exposure times of 8 (SW8), 15 (SW15) and 30 (SW30) minutes were used. Such operational parameters allow the observation of changes in the MSWI-FA and provide sustainable process conditions (energy and water consumption). The SW-treated samples were compared with i) a typical L/S = 2 water-washing for 24 h (WW) and ii) a L/S = 2 water-washing coupled with SW8 (WW + SW), to verify if a combination of both methods is feasible in view of further optimization of the steam consumption. Every sample has been replicated 3 times. The analytical data presented in the Results section is given as the means of these 3 replicates, with a standard deviation in the order of 8–10 %. The recovery rate of heavy metals after the sequential extraction procedure was in the range of 85–110 % (Matabane et al., 2021).

2.4. Major and trace element and heavy metal characterization in solid samples

The major and trace element components in raw and treated MSWI-FA were determined in bulk by Wavelength Dispersive X-Ray Fluorescence Spectrometry (WDXRF), on pressed powder pellets and using a standard-less method (semi-quantitative analysis). The loss-on-ignition (LOI) of each sample was evaluated after subjecting itto 1050 °C for 24 h in a muffle furnace. For the determination of heavy metals and remaining trace elements (Li, Ba Sr, V and Sb), the sample powders were totally digested in open Teflon beakers on a hot plate with a mixture of suprapure HF and HNO_3 (2:1 ratio). Dissolved samples were dried out and re-dissolved in a mixture of suprapure HF and HNO_3 (1:1 ratio); afterwards, they were dried out again and re-dissolved for the last time with HNO_3. The solutions obtained were analyzed by Inductively Coupled Plasma-Mass Spectrometry (ICP-MS), using a iCAPTQ ThermoFisher Scientific instruments.

2.5. Mineralogical composition

The mineralogical composition of all samples was characterized by

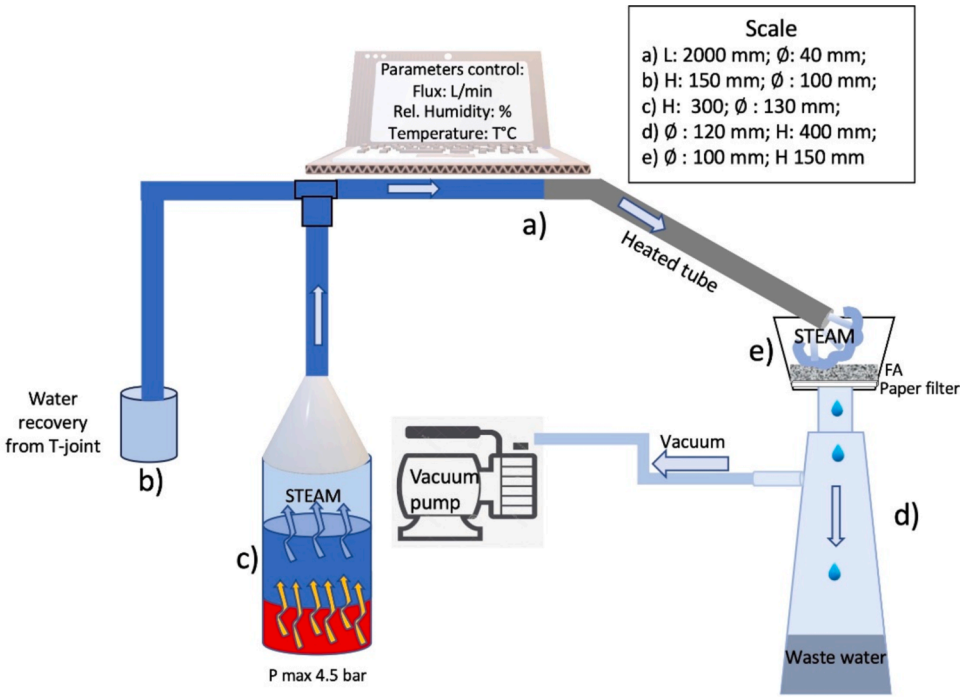

Fig. 1. Layout of the experimental apparatus for steam washing.

X-Ray Powder Diffraction (XRPD), using a Rigaku Miniflex 600, with Cu-Kα incident radiation and operating at 40 kV–15 mA. XRPD patterns were collected on pre-dried powdered samples between 3° and 70° 2θ, with a 2θ-step size of 0.02 and scan speed of 0.5°/min, using a side-loading zero-background sample holder. The amorphous and crystalline phases content was inferred by Rietveld-RIR analysis, using high purity calcined α-Al2O3 as an internal standard (10 wt%). The data refinements were carried out by the software GSASII (Toby and Von Dreele, 2013).

2.6. Elemental and isotopic analyses of total and organic carbon in solid samples

The analyses of total (TC) and organic (OC) carbon (expressed in wt %), and the relative isotope ratios ($^{13}C/^{12}C$ expressed as $\delta^{13}C_{TC}$ or $\delta^{13}C_{OC}$) were carried out by an Elemental Analyzer (EA) VarioMicro Cube (Elementar) operating in combustion mode and coupled with the Isotope Ratio Mass Spectrometer (IRMS) IsoPrime 100 (IsoPrime).

The full description of the method is provided in the Supplementary Materials. The relative isotope ratios were used only qualitatively as a fingerprint of raw and treated MSWI-FA, since a detailed investigation of C-based compounds would require more advanced mass spectrometry approaches (i.e., Py-GC/MS) (Picó and Barceló, 2022).

2.7. Leaching tests

Raw and treated MSWI-FA samples were dried for 24 h at 105 °C and then submitted to leaching tests in deionized water at L/S = 10 for 24 h, according to (EN 12457–2, 2002). The pH-dependent leaching tests were performed at 7 different pH values (4–13), according to the SW-846 Test Method 1313, after pre-titration tests to determine the acid neutralization capacity of the material (Fig. S2). After 24 h, the samples were filtered, and the liquid residues analyzed by Ion chromatography (IC), ICP-MS and pH-meter Hanna HI2211 (error ± 0.2 pH units).

2.8. Chemical analyses of leachates and wastewater

The concentration of major anions and cations were performed using a Metrohm 883 Basic IC plus instrument, with a loop of 20 µl. The calibration relied upon eight replicated analyses of the same reference sample (detection limit: 10 µg/L). Minor and trace element analyses, including heavy metals, were carried out by iCAPTQ ThermoFisher Scientific instrument.

2.9. Thermal analysis

Thermogravimetric (TG), differential thermogravimetric (DTG), and differential thermal analyses (DTA) were performed on MSWI-FA samples under a controlled air atmosphere. The analysis was performed using an STA 409 PC LUXX® Netzsch with a heating rate of 10 °C/min in an alumina crucible, ranging from room temperature (RT) up to 800 °C.

2.10. Scanning electron microscopy

Back scattered electron (BSE) images of MSWI and SW30 were collected by a JSM microscope IT300LV (JEOL USA Inc.). Typical experimental conditions were W filament, EHT 15 kV, working distance 10 mm, and standard probe current. The samples were carbon-coated prior to analysis.

2.11. Sequential extraction

The speciation distribution was determined following the five-step sequential extraction procedure described by Bernasconi et al, (2022). An adaptation to the procedure after Dematteis et al, 2023 was introduced, by increasing the acetic acid concentration in the second step. More details about the procedure are provided in the Supplementary Materials (Table S1).

2.12. Geochemical modelling

The Visual MINTEQ software, version 3.1 (Gustafsson, 2013) was employed to model the heavy metals concentration in leachates. Calculations were compared with observations from leaching tests as a function of pH. A multi-surface approach was employed to take into account heavy metal sorption/complexation on Fe/Al hydroxides (HFO)

and solid/dissolved organic matter (SOM and DOM) (Groenenberg and Lofts, 2014). The full description of the employed model is provided in the Supplementary Materials (Table S2).

3. Results

3.1. Chemical composition of raw and treated MSWI-FA

**Fig. 2 shows selected major and trace elements composition of raw and treated MSWI-FAs, determined by combining XRF (wt%) and ICP-MS (mg/kg) data, while the full dataset is shown in Table S3. The most abundant element in raw MSWI-FA is Cl (22.4 %), followed by Na (12.1 %), Ca (9.46 %), K (8.6 %), and S (3.1 %). In terms of heavy metals, a considerable amount of Zn was detected (63569 mg/kg), along with Pb (6738 mg/kg), Sb (2000 mg/kg), Cu (1797 mg/kg), and Cd (586 mg/kg).

SW induces substantial differences in the MSWI-FA chemical composition, as shown in Fig. 2. A remarkable decrease (64–90 %) of the Cl content is observable upon increasing the exposure time, (Cl = 2.4 wt % in the 30 min treated sample SW30). A similar behavior is observed for Na and K, which are reduced to 1.0 and 1.4 wt%, respectively, by SW30. This is in keeping with the weight loss that reaches 37 and 50 %, in the case of SW8 and SW30, respectively. The conventional WW provides a 50 % Cl reduction, which decreases to 2.55 wt%, if an additional SW treatment is introduced (WW + SW).

An increase in the concentrations of comparatively low water-soluble major species appears in the treated samples, mainly involving Ca, S and Si. Calcium becomes the most abundant element, accounting for up to 18–20 wt% in case of the SW15-30 treated samples (Fig. S3). Likewise, treated MSWI-FA exhibits an increase in heavy metal concentrations. Zinc almost doubles, reaching 120345 mg/kg in SW30, along with Pb, Sb, and Cu. The only exception is Cd, which markedly decreases upon increasing SW exposure time, down to 274 mg/kg. (SW30).

In raw MSWI-FA, the TC accounts for 0.51 wt%, 59 % of which is related to organic C (0.30 wt%) (Ferrari et al., 2002). By increasing SW duration, the concentrations of both TC and OC increase, reaching 1.32 and 0.54 wt% (SW30), respectively.. The isotopic ratio $\delta^{13}C$ in Table S3 of both TC and OC changes after treatment, becoming systematically "less negative" (i.e., $\delta^{13}C_{TC}$ decreases from −29.13 ‰ in MSWI-FA to −26.86 ‰ in SW30)).

3.2. Mineralogical, morphological and thermal analysis

Table 1 reports the phase composition of raw (MSWI-FA) and SW and WW treated samples. In raw fly ash, the crystalline chloride minerals (i.e., halite and sylvite) account for more than 37 wt%. Chlorine also occurs in hydrocalumite and K-tetrachlorozincate. The abundant Ca content is hosted by Ca-sulfates (i.e., anhydrite, bassanite and syngenite), along with calcite and silicate phases like melilite and merwinite. Moreover, a significant (~40 wt%) amorphous fraction is observed. The water-washing is effective in reducing the crystalline chloride content, although halite and sylvite still occur as high as 9.8 and 7.8 wt%, respectively, in combination with an increase in the less soluble amorphous phase's relative content (48 wt%). The dissolution of K-tetrachlorozincate, along with the mobilization of Cl^- and SO_4^{2-}, promotes in turn the precipitation of Zn-bearing gordaite (WW-treated MSWI-FA), though both phases occur in low amounts. SW30 causes a decrease of

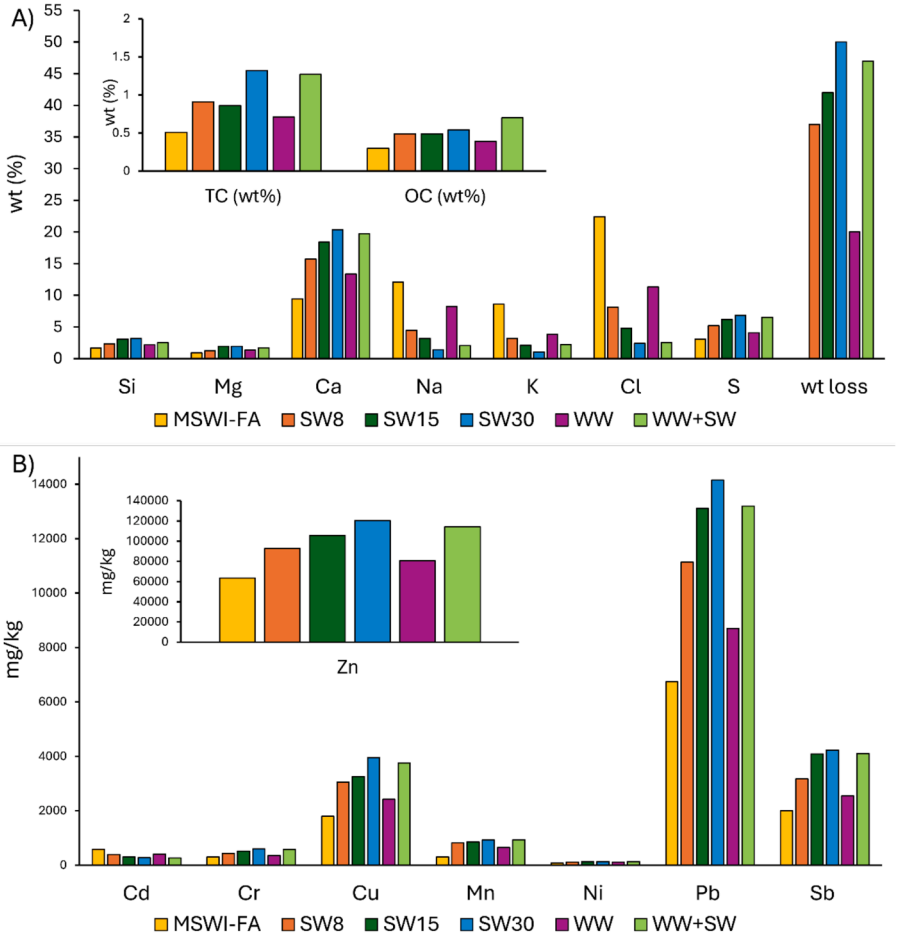

Fig. 2. Chemical composition of raw and treated MSWI-FA samples, together with the weight loss after each treatment.

Table 1
Mineralogical composition of raw (MSWI-FA) and treated samples.

Phase	Nominal formula	MSWI-FA	SW8	SW15	SW30	WW	WW + SW
Melilite	$Ca_2(Al,Mg)(Al,Si)_2O_7$	1.3	1.9	2.6	2.1	1.9	2.1
Calcite	$CaCO_3$	1.9	3.4	3.6	4.6	3.4	4.6
Quartz	SiO_2	0.6	0.8	0.8	0.9	0.7	0.9
Halite	NaCl	25.1	7.6	4.4	2.5	9.8	2.7
Hydrocalumite	$Ca_2Al(OH)_6(Cl,OH)\cdot 2H_2O$	0.5	0.8	0.9	1	0.5	1.1
Anhydrite	$CaSO_4$	11.3	17.3	16.2	18.3	7.3	4.5
Periclase	MgO	1.4	1.5	1.9	2.1	1.5	1.2
Sylvite	KCl	12.1	6.7	3.6	0.5	7.8	0.8
Ilmenite	$(Fe,Ca)TiO_3$	0.8	1.2	0.8	0.7	1	0.8
Merwinite	$Ca_3Mg(SiO_4)_2$	0.8	1.3	0.8	0.7	1.1	0.6
Bassanite	$CaSO_4\cdot 0.5H_2O$	4.5	7.2	9.3	8.4	4.2	1.4
Singenite	$K_2Ca(SO_4)_2\cdot H_2O$	0.3	0.7	1.3	0.5	0.2	–
Gypsum	$CaSO_4\cdot 2H_2O$	–	0.3	–	0.4	12.3	20.9
K-tetrachlorozincate	K_2ZnCl_4	0.5	–	–	–	–	–
Gordaite	$NaZn_4(SO_4)(OH)_6Cl\cdot 6H_2O$	–	–	–	–	0.3	–
Amorphous		38.9	49.2	53.8	57.3	48	58.5

Na-K chloride by over 90 % (Table 1). In general, the Ca-sulfate are less affected by the SW/WW treatments than chloride, although hydration reactions involving transformation of anhydrite into gypsum take place, especially in the WW and WW + SW samples, where gypsum becomes the most abundant crystalline phase. Other less-soluble phases, like calcite and melilite, increase their relative amounts after SW treatments because of the dissolution of the more soluble ones.

MSWI-FA particles exhibit heterogeneous morphology. Aggregates of small particles (<50 μm), constituted of regular habit crystals of Ca-sulfate (bladed/prismatic) and Na/K-chloride (cubic), are observable (Fig. S3). The latter can also occur as anhedral crystals, coating aluminosilicate and glass particles (Bernasconi et al, 2022). The SW-treated samples display an increase in the particle aggregation, as it is often observed in washed FA (Caviglia et al, 2022; Ferraro et al. 2019), too. Moreover, a marked decrease in salt surrounding the particles takes place because of dissolution, thus allowing the exploration of the acicular and round aggregates underneath, which are rich in Ca, Na, Al, Si and Zn (Fig. S3).

During TGA, the SW-treated samples yield weight loss fraction values of ~ 9–10 %, and the highest figure (14 %) is provided by the WW + SW treatment. In the DTA patterns (Fig. S4), an endothermic peak is observed at ~ 100 °C (water evaporation and dehydroxylation of hydrated compounds, such as bassanite and gypsum), followed by an exothermic reaction stretching up to 600 °C (combustion of organic matter), and by an endothermic transformation at 630 °C (dissociation and oxidation processes of mineral phases and alkaline compounds) (Haiying et al, 2010; Zhang et al, 2020).

3.3. Leaching tests performance and SW wastewater composition

The results of leaching tests performed on raw and SW-WW treated samples, along with the SW wastewater compositions, are set out in Table 2. The reported values were calculated by combining IC and ICP-MS measurements. Leaching tests on MSWI-FA showed a very high concentration of chloride (over 17000 mg/L), much above the legal threshold for non-hazardous waste (2500 mg/L), while sulfate remained within the legal limit (Table 2) (Ministerial Decree, 2010). As for heavy metals, leaching of Zn, Cr, Pb, Cu, Mo, Cd and Sb was detected, although only for Cd and Sb, the measured values exceeded the legal thresholds (1.341 against 0.1 and 1.24 against 0.07 mg/L, respectively). WW leads to a general decrease in leaching from all of the investigated heavy metals, most notably Cd, that drops to 0.023 mg/L, whereas chloride remains quite high (9260 mg/L). SW effectively reduces both heavy metal and chloride leaching. Cd is no longer detected in samples from SW8 treatment, and the minimum leaching observable is obtained by SW30, in particular for Zn, Cr and Pb. A similar trend is shared by Cl^-, which reaches 2280 mg/L (Table 2). Sb leaching, though reduced by 70 %, still remains over the legal limit (0.386 mg/L). In the case of SW +

Table 2
Leaching tests performance and SW-wastewater compositions.

	Leaching tests							*Wastewater*		
	MSWI-FA	SW8	SW15	SW30	WW	WW + SW	Limits	SW8	SW15	SW30
pH	7.5	7.8	8.1	8.2	7.8	8.1	5–12	6.3	6.3	6.3
LS ratio	10	10	10	10	10	10		1.1	1.5	2.2
Chloride (mg/L)	17225	8088	4150	2280	9260	2363	2500	>70000	>70000	>70000
Sulfate (mg/L)	3767	2900	2630	2514	3120	2470	5000	5310	5583	5479
Li (mg/L)	4.213	1.915	0.513	0.643	1.715	0.318		15.33	21.34	24.29
Ti (mg/L)	0.675	<d.l.	0.413	0.256	<d.l.	0.152		0.698	0.744	0.702
V (mg/L)	0.002	<d.l.	<d.l.	<d.l.	<d.l.	<d.l.		<d.l.	<d.l.	<d.l.
Cr (mg/L)	0.383	0.305	0.194	0.147	0.312	0.159	1	0.049	0.268	0.329
Mn (mg/L)	0.002	<d.l.	<d.l.	<d.l.	<d.l.	<d.l.		1.309	0.787	0.757
Co (mg/L)	0.001	<d.l.	<d.l.	<d.l.	<d.l.	<d.l.		0.007	0.003	0.003
Ni (mg/L)	<d.l.	<d.l.	<d.l.	<d.l.	<d.l.	<d.l.	1	0.043	0.042	0.083
Cu (mg/L)	<d.l.	<d.l.	<d.l.	<d.l.	<d.l.	0.007	5	1.145	1.044	0.712
Zn (mg/L)	0.809	0.41	0.103	0.025	0.561	0.021	5	6010.3	7204.4	3467.2
As (mg/L)	0.003	0.005	0.004	0.003	0.006	0.003	0.2	<d.l.	<d.l.	<d.l.
Mo (mg/L)	0.292	0.305	0.408	0.476	0.325	0.456	1	<d.l.	<d.l.	<d.l.
Sr (mg/L)	1.336	1.613	3.326	2.889	1.693	2.935		1.544	1.413	1.459
Cd (mg/L)	1.341	<d.l.	<d.l.	<d.l.	0.023	<d.l.	0.1	327.2	267.5	201.1
Sb (mg/L)	1.240	0.482	0.410	0.386	0.566	0.431	0.07	0.612	0.938	0.493
Ba (mg/L)	0.496	0.140	0.143	0.200	0.352	0.131	10	0.834	1.630	1.390
Pb (mg/L)	0.311	0.094	0.020	<d.l.	0.136	<d.l.	1	367.5	471.1	269.7

WW, results similar to those from SW30 are achieved.

The pH of wastewater from SW is very close to the deionized water's (6.3) (Table 2). In the case of heavy metals, the largest values were observed for Zn (3000–7000 mg/L), Pb (270–470 mg/L), and Cd (201–270 mg/L), while relevantly lower concentrations were measured for Cr, Cu and Sb, (0.04–0.334, 0.714–1.052 and 0.493–0.956 mg/L, respectively). The general decrease in the measured concentrations of SW30 is probably attributable to the relatively higher volume of wastewater, which, as it will be discussed below, can be likened to an equivalent L/S ratio of ~ 2.2.

A mass balance of the heavy metals investigated was calculated, and the results are set out in Table 3; details are reported in the Supplementary Materials (Table S4-6). The SW treatment affected the heavy metals resilience capacity in different ways. Cadmium is the most SW sensitive, as proven by the fact that SW30 provides a removal rate of 75 % (against an overall removal of 12 %), followed by Zn, whose leaching decreases by 13.5 and 17 %, for SW8 and SW15, respectively. Pb follows, but at a lower removal rate (6–10.5 %). Finally, Cr, Cu, and Sb, exhibit comparatively modest removal rates, in the range 0.03–0.2 %.

3.4. Heavy metals speciation distribution

The results of a 5-step sequential extraction are shown in Fig. 3: on the left, the relative contributions (%) of each fraction with respect to the total heavy metal content are shown. In raw MSWI-FA, most heavy metals are associated with easily soluble/exchangeable (F1) and acid-soluble (F2) fractions (Bernasconi et al, 2022; Thong et al, 2020). F2 accounts for 63, 48 and 45 % of the total Zn, Pb and Cu amounts, respectively. Their F1 component is very limited in all the investigated heavy metals (around 0.4 %; not noticeable in Fig.), except in Cd, where it becomes preponderant (65 %). Copper also shows a significant association with the oxidizable F4 (28 %), i.e., oxidizable compounds like organic matter and sulfide (Bernasconi et al, 2022; Thong et al, 2020). A similar speciation is exhibited by Cr (20 %), although for this element the most important association is with the reducible F3 (30 %) and residual F5 (46 %) fractions. As for Sb, F5 accounts for 53 %, followed by F3, F2, and F4, with values of 20, 15 and 12 %, respectively. The comparison with the treated samples demonstrates that the speciation distribution of almost all the investigated heavy metals is modified by SW. Cd displays a dramatic depletion of F1 (from 65 % to 0.2 %), leading to a significant relative enrichment in the other speciation fractions. Zinc presents a weakly varying trend of F2, with values of 53, 46, and 48 % for 8–15-30 min treatment, respectively, in combination with the absence of F1 and an increase of F5 speciation (from 12 % to 25–30 %). Conversely, F2 accounts for 30–35 % of the content of Pb in the treated samples, while F5 changes from 15 to 28–30 %. In addition, the association of Pb with Fe/Mn oxyhydroxides (F3) increases up to 30 %. In the case of Cu, SW promotes reductions of F2 and F4, from 45 to 37–38 % and from 28 to 19–20 %, respectively. Similarly, the Cr F4 speciation decreases from 20 to 12–13 %, while F3 increases to 38–40 % of total Cr in SW15-30 samples. Finally, the speciation distribution of Sb does not show significant modifications after washing treatment, as F1 remains ~ 0.2 % and F4 slightly decreases down to 8 %.

3.5. pH-dependent leaching tests and geochemical modelling of MSWI-FA

The comparison between experimental leaching results and modelling at pH 4–13, in the case of the most abundant heavy metals in raw MSWI-FA (i.e. Zn, Pb, Cu, Cd, Cr and Sb), is presented in Fig. 4. The concentration trends as a function of pH are similar to the ones of other industrial solid wastes, where amphoteric behaviors (i.e. maximum leaching at acidic pH, which decreases to a minimum value with increasing pH and then increases again at alkaline pH) are often observed (Dijkstra et al, 2006; Liu et al, 2023; Meima et al, 1996).

Zn, Cd and Cu are significantly dissolved (85, 90 and 65 %, respectively) at pH ~ 4–5, while an important retention in the solid takes place at pH ~ 8–10, as their concentration in solution drops by 3–4 orders of magnitude. At higher pH values, their dissolution increases, up to 2 orders of magnitude at pH 12.5–13. Pb, Cr and Sb are extracted into solution at pH ~ 4, with values of 20, 0.1 and 2 %, respectively. In the former case, the leaching concentration decreases gradually for pH 5 → 9 and increases at higher pH values. For Cr and Sb, the dissolved amount remains relatively stable up to pH ~ 9, decreases at pH ~ 10–11, and slightly increases at pH ~ 13. Similar trends as a function of pH are obtained for SW30, albeit with concentration values generally lower than raw MSWI-FA.

The simulated leaching concentration *versus* pH is shown in Fig. 4 (left), where a good match with the experimental profile is visible for most metals. In case of Zn and Cd, dissolution/precipitation reactions are governed by $ZnCO_3$ and $CdCO_3$ (otavite) at pH ~ 5–10, and by Zn $(OH)_2$ and $Cd(OH)_2$ at pH > 9–11. The adsorption on HFO represents the main mechanism that controls leaching at pH <5 (Dijkstra et al, 2006; Tiberg et al, 2021). Lead solubility is controlled by sulfate at acidic and alkaline pH, in the form of $PbSO_4$ and $Pb_4(OH)_6(SO_4)_2$, respectively. At intermediate pH values (i.e., ~6–10), cerussite ($PbCO_3$) becomes the most stable phase (Keim et al, 2015). Cr and Cu oxides (Cr_2O_3, CuO) are the solubility-controlling phases for such species at alkaline pH, while adsorption on HFO and SOM surfaces plays an important role a pH ~ 4–9, though the overestimation of Cr leaching at pH <6 hints that other processes occur, possibly involving redox reactions (Fig. S5) (James, 1996). The antimony trend is well modelled by the equilibrium solubility of $Ca_2Sb_2O_7$ (romeite) at pH ~ 5–9, but it is significantly overestimated at higher pH values.

Table 3
Removal rate (%) of MSWI-FA heavy metals after SW.

	Cr	Cu	Zn	Cd	Sb	Pb
SW8	0.02	0.07	10.4	61.0	0.03	6.0
SW15	0.14	0.09	17.1	68.2	0.07	10.5
SW30	0.25	0.09	12.1	75.1	0.05	8.8

4. Discussion

4.1. Chlorine

Chlorine in MSWI-FA mostly occurs in crystalline chloride and less soluble, complex minerals, such as hydrocalumite (Wang et al, 2023). The former phases are particularly abundant (around 37 wt%, Table 2) and are largely affected by SW. Previous studies showed that an increase in water temperature in washing treatments does not significantly improve the efficacy of chloride dissolution, while the L/S ratio is more effective (Caviglia et al, 2022; Ferraro et al. 2019). A water balance was estimated for SW30. On average, the steam mass balance indicates that around 0.2 wt% is retained by MSWI-FA surfaces, 5.5 wt% is collected as wastewater, 56 wt% is dispersed and 38 wt% is condensed in the T-joint. This is equivalent (on 10 g MSWI-FA) to an "*effective*" L/S ratio of ~ 1.1, 1.5 and 2.5, for 8, 15 and 30 min, respectively. From SW8 to SW30 the efficiency of chloride removal improves up to over 90 % (Table S1 and 1), i.e., Cl leaching lies below the legal limits for non-hazardous waste (Table 2). At the same time, hydrocalumite increases in content after treatment, because its solubility is significantly dependent on pH (<5–5.5), while the wastewater is only slightly acidic (pH 6.3) (Wang et al., 2023).

4.2. Heavy metals

The characterization of raw MSWI-FA showed that the most abundant heavy metals (Zn, Cd, Cu, Pb) are associated with easily soluble/exchangeable (F1) and acid-soluble (F2) fractions (Fig. 3), which further confirms the hazardousness of the waste, as these fractions are prone to easily leach out pollutants into the environment (Bernasconi et al, 2022;

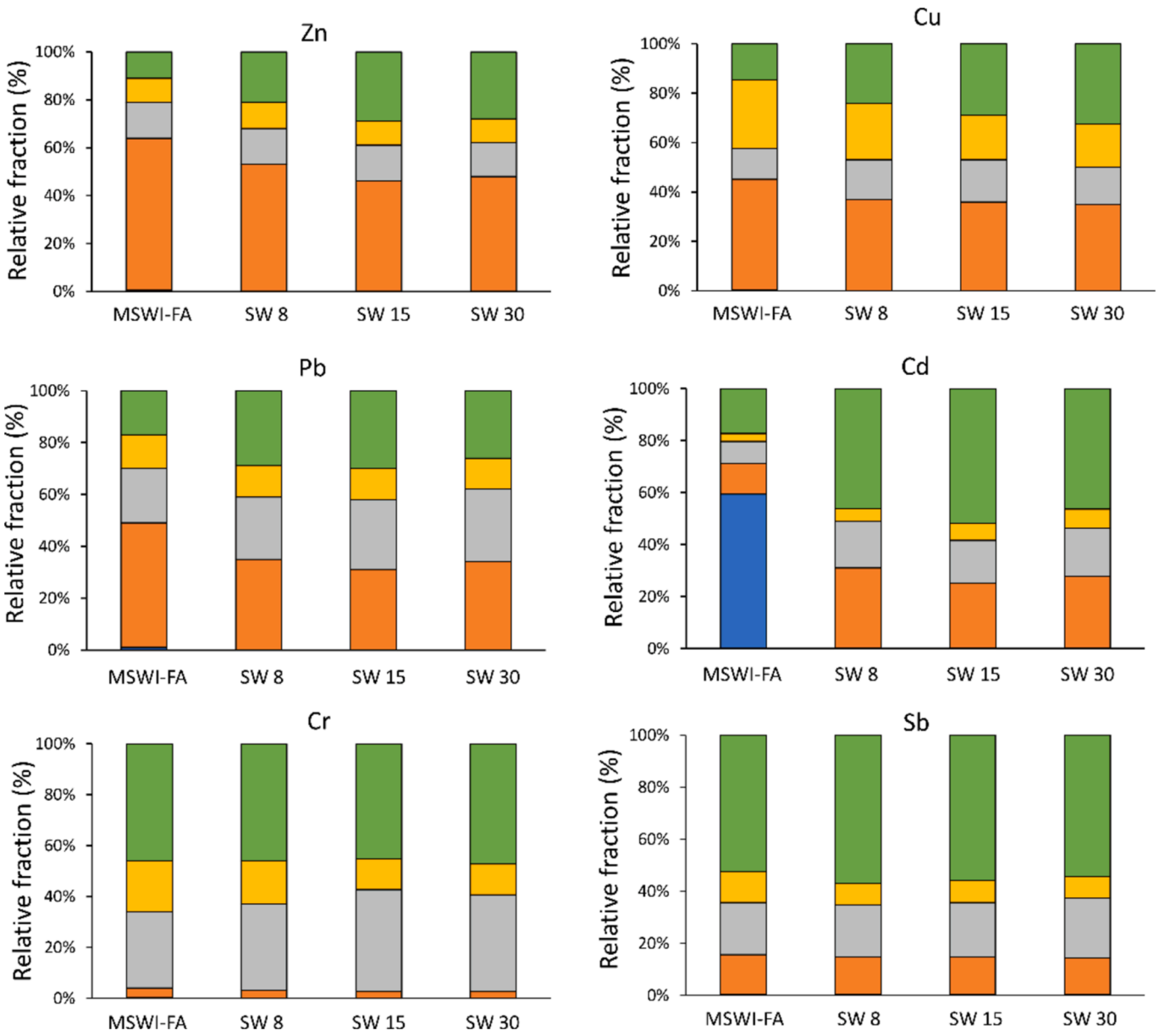

Fig. 3. Heavy metals 5-step sequential extraction of raw and treated MSWI-FA. Blue: F1 (soluble/exchangeable); Orange: F2 (acid-soluble); Grey: F3 (reducible); Yellow: F4 (oxidizable); Green: F5 (residual).

Thong et al, 2020). The mass balance in Table 3 demonstrates that SW can remove part of these heavy metals; the results in Fig. 3 show that the SW treatment has also an impact on the speciation distribution, even for those heavy metals not affected by a decrease in total mass. For Cd, the removal is related to the actual dissolution of F1, since its relative abundance in MSWI-FA is very close to the weight loss estimated by the mass balance (i.e., 65 % against 60–75 %, Table 3). $CdCl_2$ and CdClOH were proposed as Cd-bearing phases in this system, and the geochemical model at the treatment pH conditions (between 6–8) indicates significant undersaturation of these phases i.e., high solubility (calculated saturation index of −4.5 and −3.2, respectively) (Zhang et al., 2008). Moreover, although soluble $ZnCl_2$ and $PbCl_2$ may be present, the removal rate of Zn and Pb in Table 3 largely exceeds their relative F1 abundance, thus suggesting that other fractions are also involved(i.e. 6–10 % against 0.5 %, for Pb). The speciation distribution in SW samples indicates a reduction of F2 (Fig. 3), and in fact Zn/Pb carbonates and hydroxides are supposed to be solubility-controlling phases at intermediate pH values (Fig. 4). The slightly acidic condensed water from SW on the MSWI-FA surface may favor the partial dissolution of this fraction (Qin et al., 2023; Weibel et al., 2018). The pH-dependent leaching tests clearly show that a significant release of Zn and Pb is achieved at pH <6.5–7, although a much longer contact time is required (48 h). This effect is promoted by the concomitant dissolution of chlorides on the surface of the aggregates, so that the heavy metals bearing small particles underneath (see Fig. S3) are exposed. Indeed, high concentrations of Zn and Pb are detected in wastewater (Table 2). In addition, the increase of the F3 and F5 fractions hints that reprecipitation reactions into more stable compounds also occur, which may explain the reduced removal rate in SW30 with respect to SW15 (Table 3). A similar process is probably involved in the case of Cr and Cu, even though only a small fraction is removed (<0.3 %). At this pH, although H^+ ions exhibit the strongest binding affinity for the negatively charged Fe/Al oxyhydroxide binding sites, their competition with other cations remains relatively limited. As a result, the interaction of the latter with the binding sites is favored, occurring either through single-site or dual-site binding modes. (Hiemstra and van Riemsdijk, 1996, 2006). An analogue increase in the

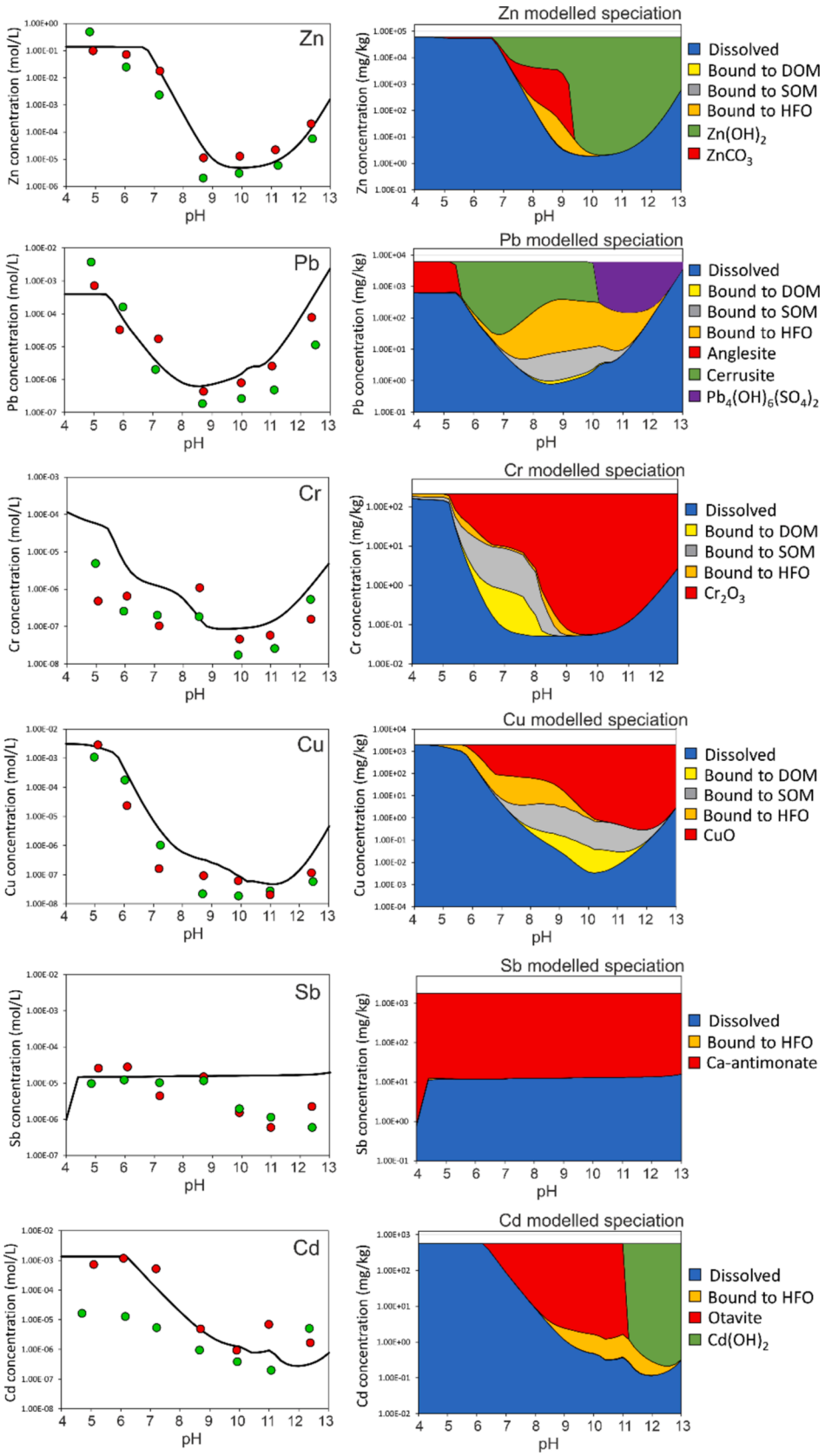

Fig. 4. Measured pH-dependent leaching concentrations of selected heavy metals of MSWI-FA (red dots) and SW30 (green dots), together with the simulated profile of raw MSWI-FA (black line) (left). Modelled heavy metals speciation at equilibrium conditions (right).

adsorbed speciation was observed for most heavy metals after microwave-assisted washing and attributed to the mobilization of the carbonate-bound fraction(Wang et al., 2023).

No appreciable change was revealed in Sb speciation. The model suggests romeite as the main hosting-phase (Fig. 4), whose solubility is not affected by pH in the range 5–13, while the observed drop at pH > 9 is possibly related to coprecipitation with ettringite ($Ca_6Al_2(SO_4)_3(OH)_{12}{\cdot}26H_2O$), a common mineral controlling the solubility of Ca and sulfate at pH > 10 (Meima et al., 1998). The calculation of the romeite saturation index in SW15 wastewater results in a value close to precipitation equilibrium (−0.35, Table S7), which further supports the correlation between Sb leaching and Ca availability. This behavior may explain the residual Sb leaching observed in Table 2. To further limit Sb release, it is necessary to couple SW with another treatment, by introducing, for instance, a reducing agent (i.e., Fe^0 or Fe^{2+} salt) such that Sb (V) → Sb(III), whose solid phases are characterized by very low solubility (Meima et al., 1998; Wang et al, 2019).

4.3. Carbon

A significant increase in TC and OC contents signatures for all the SW-treated samples (Fig. 2), with respect to MSWI-FA, points to the occurrence of an organic carbon fraction weakly affected by the SW. This is confirmed by the negative $^{13}C/^{12}C$ values, which are typical of organic matter (Wagner et al., 2018). Interestingly, negative signatures were obtained from analyzing the SW-treated samples both at T <500 °C (for OC analyses) and at T > 500 °C (for TC analyses), where 500 °C is considered the maximum temperature for the stability of organic compounds (Natali et al., 2018). In particular, the TC isotopic values are slightly more negative than the OC isotopic values, indicating the persistence of organic matter with a strong negative signature, even after the combustion at > 500 °C. We took into consideration the presence of organic humic-like substances, whose aromatic structures are thermically stable up to 700 °C (Danilin et al., 2023).

Previous studies showed that fulvic-like and humic-like substances may be present in MSWI-FA and be partially responsible for the mobilization of heavy metals due to adsorption/complexation reactions through carboxyl/phenolic moieties (Dijkstra et al., 2006; Liu et al., 2022). The model in Fig. 4 highlights that Cu and Cr interaction with organic matter in raw MSWI-FA takes place also in solution, where ~ 70–90 % of the dissolved species is complexed by DOM at pH ~ 7–8 and 8–10, respectively. Although a detailed investigation of the organic matter is outside the scope of this work, it seems reasonable to suggest that some degree of dissolution/oxidation occurs, while the associated heavy metals either reprecipitate or are adsorbed into/onto Fe/Al oxyhydroxides (i.e., F3) (Liu et al., 2022; Wang et al., 2023). This may explain the reduced release of Cr, reported in Table 2.

4.4. Final implications for MSWI-FA treatment

When compared with the conventional WW, a general improvement is already achieved by SW8, both in terms of chloride and heavy metal leaching (Table 2). The short exposure time, along with the low volume of water involved, favors a kinetic-driven process, similarly to what has been observed in a previous work about multiple-step washing (Caviglia et al, 2022).

Overall, the SW treatment can be likened to a desalination/dechlorination process, promoted by dissolution of chlorides that cover the larger FA-particles, in combination with the mechanical removal of the very fine particles. This washing process is also promoted by high temperature, which has been observed to improve the dissolution kinetics of heavy metals-bearing phases in similar systems (Caviglia, 2022). This was sufficient to bring most of the heavy metals below their legal leaching, the impact on heavy metals speciation was confined by the use of steam/water at natural pH (i.e., not acidic). This is demonstrated by the similarity of the pH-dependent leaching profiles of raw and treated MSWI-FA (Fig. 4).. Even though a partial removal and conversion from F2 (carbonates/hydroxides) to F3 (adsorbed) was observed in the speciation distribution of most heavy metals (Fig. 3 and Table 3), the leaching mechanisms at (pseudo)equilibrium conditions are not markedly altered by the treatment. Generally, the water-based methods are known to be less effective than other strategies in eliminating heavy metals (Ferraro et al., 2019; Qin et al., 2023). In particular, the FLUWA/FLUREC process and thermal treatments have demonstrated to accomplish a remarkable removal and recovery rate for Zn, Pb and Cd (up to 99 %), through an acidic leaching coupled with electrowinning and metal-rich vapour condensation (Zhang et al., 2021). Although these approaches are better suited to achieving a true valorization of MSWI-FA and may reach a positive environmental impact, their implementation suffers from their significant cost. The former is economically feasible only for ashes with very high content of metals (i.e, > 40000 mg/kg of Zn), as a huge amount of acid is used to neutralize the significant alkalinity of MSWI-FA (Fellner et al., 2015; Huber et al., 2018). The latter employs high temperature regimes (between 900–1300 °C) (Huber et al., 2018; Zhang et al., 2021).

For these reasons, the stabilization/solidification with binders followed by controlled landfilling remains the most popular strategy (Li et al., 2024). In this context, SW may offer an alternative to water washing as a pretreatment to reduce the chloride content, which is known to negatively impact on the hydration reactions of the commonly used Portland cement (Aubert et al., 2006; Liu et al., 2022; Li et al., 2024). Washing pretreatment is also performed before clinkering co-combustion to obtain eco-cement clinker (Zhang et al., 2021). Moreover, the highly concentrated wastewater may provide a valuable source for the recovery of metals and salt, as illustrated in Fig. 5 (Date et al, 2024).

Although an in-depth Life-Cycle-Assessment is outside the scope of this work, effectively implementing the SW approach would yet require a thorough evaluation of two key factors: the potential revenue loss from diverting a portion of the steam typically used for electricity generation, and the cost savings associated with managing less hazardous waste (Huber et al., 2018). These factors further depend on the balance between the energy spent generating the steam and the energy recovered by the electricity cogeneration system, weighted by the electricity value in the municipality where the WtE plant is located (Cherubini et al, 2009; Anshassi et al, 2021).

Preliminary estimation suggests that less than 1 wt% of the steam produced by the plant in a year would be required to treat the mass of MSWI-FA generated in the same timeframe, according to the most drastic conditions studied (i.e., SW30). This figure may vary greatly between different plants and countries, where, in addition, MSWI residues with very different physicochemical characteristics are generated (Ferraro et al, 2019; Funari et al. 2023). Indeed, although the main mechanisms of SW as described in the previous sections are expected to be reproducible, the unusually high chloride/heavy metal content and low basicity of the MSWI-FA employed in this study (possibly due to a waste feed rich in unsorted kitchen waste, wood and PVC), along with the absence of neutralization compounds more typically found in air pollution control residue (i.e., CaClOH, $Ca(OH)_2$), limit the direct extension of the quantitative results to all types of ashes (Zhang et al., 2021; Wolffers et al., 2021). Based on the setup layout (Fig. 1) and water balance in section 4.1, a partial recovery of energy and mass from the dispersed steam during the exposure time of SW can be envisaged through an optimization of the system, in combination with the recyclability of the condensed steam in the T-joint. Moreover, a two-step treatment based on water and steam washing, as shown here, might provide an additional viable solution for optimizing the exploited steam, thus improving the feasibility and scalability of the process.

5. Conclusions

The study highlights the potential of steam washing (SW) as an

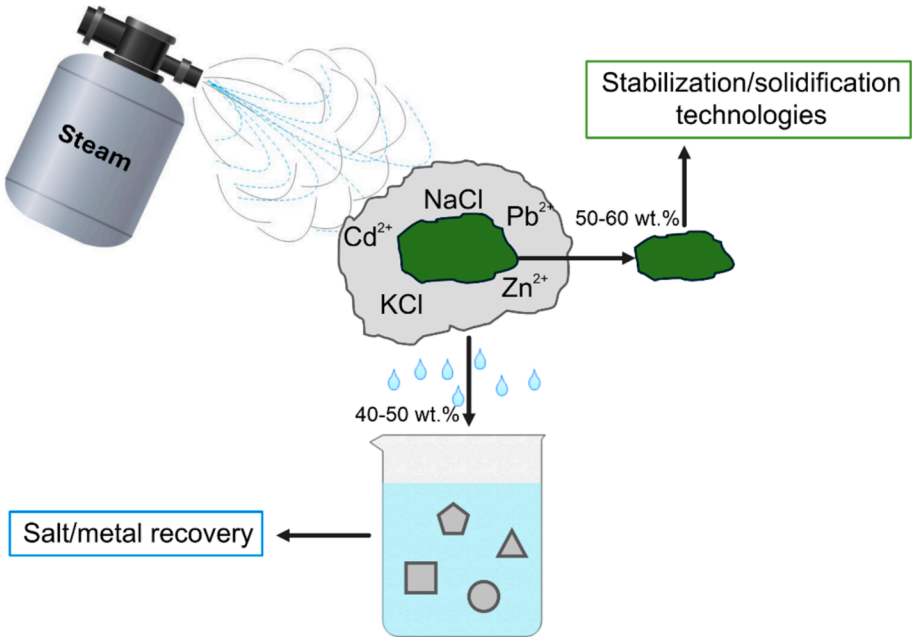

Fig. 5. Outline of the steam washing treatment.

effective dechlorination pretreatment for managing municipal solid waste incineration fly ash (MSWI-FA). A detailed analytical investigation as a function of exposure time showed that SW improves chloride removal efficiency significantly with respect to conventional water washing, achieving over 90 % under optimal conditions (30 min), with chloride and most heavy metals leaching reduced below legal thresholds for non-hazardous waste. SW also facilitates partial heavy metal removal, particularly for Cd (61–75 %), Zn (10–17 %), and Pb (6–10 %), by promoting the dissolution of soluble fractions (F1 and F2) and inducing reprecipitation/adsorption into more stable compounds (F3 and F5). However, the treatment's impact on heavy metal content is limited by its natural pH, making it less effective than acidic leaching methods. In particular, geochemical modelling indicates that Sb behavior is dependent on its oxidation state as Sb(V), therefore additional reducing treatments are required, to transform it into the less mobile Sb(III).

Overall, preliminary results suggest that less than 1 % of a waste-to-energy plant's annual steam output is sufficient to treat its MSWI-FA, implying reasonable feasibility with optimization. The concentrated wastewater from SW offers additional opportunities for resource recovery, including salts and metals, which could enhance economic viability.

Future research should address the variability in MSWI-FA compositions, as differences in waste streams and plant collection strategies may affect the treatment outcomes. Furthermore, a detailed life-cycle assessment is crucial to evaluating the environmental and economic trade-offs of SW implementation. System optimization, such as improving steam recovery and combining water and steam washing, could improve efficiency and scalability. This, together with the low volume of wastewater produced and the exploitation of a commodity already available at the incineration plant, may position SW as a sustainable alternative in MSWI-FA management strategies.

CRediT authorship contribution statement

Davide Bernasconi: Writing – review & editing, Writing – original draft, Visualization, Validation, Methodology, Investigation, Formal analysis, Data curation, Conceptualization. **Caterina Caviglia:** Writing – review & editing, Visualization, Methodology, Investigation, Conceptualization. **Enrico Destefanis:** Writing – review & editing, Visualization, Methodology, Investigation, Funding acquisition, Data curation, Conceptualization. **Costanza Bonadiman:** Writing – review & editing, Resources, Project administration, Methodology, Investigation, Funding acquisition. **Valentina Brombin:** Writing – review & editing, Methodology, Investigation. **Maura Mancinelli:** Writing – review & editing, Visualization, Investigation. **Renzo Tassinari:** Investigation. **Alessandro Pavese:** Writing – review & editing, Supervision, Resources, Project administration, Funding acquisition, Conceptualization.

Funding

The present study (AP) has been partly funded by Ministero della Transizione Ecologica through the call: "CLEAN – Ceneri Leggere Eco-sostenibili per un Ambiente No-rifiuti" (m_amte.MiTE.REGISTRO UFFICIALE.USCITA.0049573.22-04-2022).

Declaration of competing interest

The authors declare that they have no known competing financial interests or personal relationships that could have appeared to influence the work reported in this paper.

Acknowledgments

This manuscript also benefited from language comments and suggestions of Barbara Galassi.

Appendix A. Supplementary data

Supplementary data to this article can be found online at https://doi.org/10.1016/j.wasman.2025.01.031.

Data availability

Data will be made available on request.

References

Anshassi, M., Sackles, H., Townsend, T.G., 2021. A review of LCA assumptions impacting whether landfilling or incineration results in less greenhouse gas emissions. Resour. Conserv. Recycl. 174, 105810. https://doi.org/10.1016/j.resconrec.2021.105810.

Aubert, J.E., Husson, B., Sarramone, N., 2006. Utilization of municipal solid waste incineration (MSWI) fly ash in blended cement: Part 1: Processing and characterization of MSWI fly ash. J. Hazard. Mater. 136, 624–631. https://doi.org/10.1016/j.jhazmat.2005.12.041.

Bernasconi, D., Caviglia, C., Destefanis, E., Agostino, A., Boero, R., Marinoni, N., Bonadiman, C., Pavese, A., 2022. Influence of speciation distribution and particle size on heavy metal leaching from MSWI fly ash. Waste Manag. 138, 318–327. https://doi.org/10.1016/j.wasman.2021.12.008.

Bernasconi, D., Viani, A., Zárybnická, L., Mácová, P., Bordignon, S., Das, G., Borfecchia, E., Štefančič, M., Caviglia, C., Destefanis, E., Bernasconi, A., Gobetto, R., Pavese, A., 2023a. Reactivity of MSWI-fly ash in Mg-K-phosphate cement. Constr Build Mater. 409, 134082. https://doi.org/10.1016/j.conbuildmat.2023.134082.

Bernasconi, D., Viani, A., Zárybnická, L., Mácová, P., Bordignon, S., Caviglia, C., Destefanis, E., Bernasconi, A., Gobetto, R., Pavese, A., 2023b. Phosphate-based geopolymer: Influence of municipal solid waste fly ash introduction on structure and compressive strength. Ceram. Int. 49 (13), 22149–22159. https://doi.org/10.1016/j.ceramint.2023.04.042.

Caviglia, C., Destefanis, E., Pastero, L., Bernasconi, D., Bonadiman, C., Pavese, A., 2022. MSWI Fly Ash Multiple Washing: Kinetics of Dissolution in Water, as Function of Time. Temperature and Dilution, Minerals 12, 742. https://doi.org/10.3390/min12060742.

Chen, J., Fu, C., Mao, T., Shen, Y., Li, M., Lin, X., Li, X., Yan, J., 2022. Study on the accelerated carbonation of MSWI fly ash under ultrasonic excitation: CO2 capture, heavy metals solidification, mechanism and geochemical modelling. Chem. Eng. J. 450, 138418. https://doi.org/10.1016/j.cej.2022.138418.

Chen, X., Bi, Y., Zhang, H., Wang, J., 2016. Chlorides removal and control through water-washing process on MSWI fly ash. Procedia Environ. Sci. 31, 560–566. https://doi.org/10.1016/j.proenv.2016.02.086.

Cherubini, F., Bargigli, S., Ulgiati, S., 2009. Life cycle assessment (LCA) of waste management strategies: Landfilling, sorting plant and incineration. Energy 34, 2116–2123. https://doi.org/10.1016/j.energy.2008.08.023.

Cialani, C., Mortazavi, R., 2020. The Cost of Urban Waste Management: An Empirical Analysis of Recycling Patterns in Italy. Front. Sustain. Cities 2, 8. https://doi.org/10.3389/frsc.2020.0000.

Danilin, I., Tolpeshta, I., Izosimova, Y., Pozdnyakov, L., Stepanov, A., Salimgareeva, O., 2023. Thermal Stability and Resistance to Biodegradation of Humic Acid Adsorbed on Clay Minerals. Minerals 13, 1310. https://doi.org/10.3390/min13101310.

Date, M., Jaspal, D., 2024. Dyes and heavy metals: removal, recovery and wastewater reuse—a review. Sustain. Water Resour. Manag. 90. https://doi.org/10.1007/s40899-024-01073-8.

Destefanis, E., Caviglia, C., Bernasconi, D., Bicchi, E., Boero, R., Bonadiman, C., Confalonieri, G., Corazzari, I., Mandrone, G., Pastero, L., Pavese, A., Turci, F., Wehrung, Q., 2021. Valorization of mswi bottom ash as a function of particle size distribution, using steam washing. Sustainability (switzerland) 12, 11–17. https://doi.org/10.3390/su12229461.

De Matteis, C., Mantovani, L., Tribaudino, M., Bernasconi, A., Destefanis, E., Caviglia, C., Toller, S., Dinelli, E., Funari, V., 2023. Sequential extraction procedure of municipal solid waste incineration (MSWI) bottom ash targeting grain size and the amorphous fraction. Front. Environ. Sci. 11, 1254205. https://doi.org/10.3389/fenvs.2023.1254205.

Dijkstra, J.J., Van Zomeren, A., Meeussen, J.C.L., Comans, R.N.J., 2006. Effect of Accelerated Aging of MSWI Bottom Ash on the Leaching Mechanisms of Copper and Molybdenum. Environ. Science & Tech. 40, 4481–4487. https://doi.org/10.1021/es052214s.

EN 12457-2:2002 – Characterisation of waste – Leaching – Compliance test for leaching of granular waste materials and sludges – Part 2: One stage batch test at a liquid to solid ratio of 10 l/kg for materials with particle size below 4 mm (without or with size reduction). https://standards.iteh.ai/catalog/standards/sist/fc48477e-aad3-45a2-8ca8-52bc2a94cfcc/sist-en-12457-2-2004.

European Committee for Standardization, 2006. CEN/TR 15310-1 characterisation of waste—sampling of waste materials—part 1: guidance on selection and application of criteria for sampling under various conditions. In: European Committee for Standardization, Brussels. ICS:13.030.10, 13.030.20.

Eurostat. *Treatment of waste-by-waste category, hazardousness, and waste management operations - Eurostat.* 2021. url: https://ec.europa.eu/eurostat/web/products-datasets/- /env_wastrt.

Ferrari, S., Belevi, H., Baccini, P., 2022. Chemical speciation of carbon in municipal solid waste incinerator residues. Waste Manag 22, 303–314. https://doi.org/10.1016/S0956-053X(01)00049-6.

Ferraro, A., Farina, I., Race, M., Colangelo, F., Cioffi, R., Fabbricino, M., 2019. Pre-treatments of MSWI fly-ashes: A comprehensive review to determine optimal conditions for their reuse and/or environmentally sustainable disposal. Rev. Environ. Sci. Biotechnol. 18, 453–471. https://link.springer.com/article/10.1007/s11157-019-09504-1.

Fellner, J., Lederer, J., Purgar, A., Winterstetter, A., Rechberger, H., Winter, F., Laner, D., 2015. Evaluation of resource recovery from waste incineration residues – The case of zinc. Waste Manag. 37, 95–103. https://doi.org/10.1016/j.wasman.2014.10.010.

Funari, V., Toller, S., Vitale, L., et al., 2023. Urban mining of municipal solid waste incineration (MSWI) residues with emphasis on bioleaching technologies: a critical review. Environ Sci Pollut Res 30, 59128–59150. https://doi.org/10.1007/s11356-023-26790-z.

Groenenberg, J.E., Lofts, S., 2014. The use of assemblage models to describe trace element partitioning, speciation, and fate: a review. Environ. Toxicol. Chem. 33, 2181–2196. https://doi.org/10.1002/etc.2642.

Ministerial Decree, G.U., December 2010. 27/09/2010-Definition of the Criteria of Admissibility of Landfill Waste. Available online: Serie Generale n-281. 1 https://www.gazzettaufficiale.it/eli/id/2010/12/01/10A14538/sg.

Gustafsson J.P. 2013 Visual MINTEQ 3.1. http://vminteq.lwr.kth.se/.

Hiemstra, T., van Riemsdijk, W.H., 2006. On the relationship between charge distribution, surface hydration, and the structure of the interface of metal hydroxides. J. Colloid Interf. Sci. 301, 1–18. https://doi.org/10.1016/j.jcis.2006.05.008.

Hiemstra, T., van Riemsdijk, W.H., 1996. A surface structural approach to ion adsorption: the charge distribution (CD) model. J. Colloid Interf. Sci. 179, 488–508. https://doi.org/10.1006/jcis.1996.0242.

Huber, F., Laner, D., Fellner, J., 2018. Comparative life cycle assessment of MSWI fly ash treatment and disposal. Waste Manag 73, 392–403. https://doi.org/10.1016/j.wasman.2017.06.004.

James, B.R., 1996. The challenge of remediating chromium-contaminated soil. Environ. Sci. Technol. 30, 248A–251A. https://doi.org/10.1021/es962269h.

Kanhar, A.H., Chen, S., Wang, F., 2018. Incineration Fly Ash and Its Treatment to Possible Utilization: A Review. Energies 13, 6681. https://doi.org/10.3390/en13246681.

Keim, M.F., Markl, G., 2015. Weathering of galena: Mineralogical processes, hydrogeochemical fluid path modeling, and estimation of the growth rate of pyromorphite. Am. Min. 100, 1584–1594. https://doi.org/10.2138/am-2015-5183.

Li, W., Li, L., Wen, Z., Yan, D., Liu, M., Huang, Q., Zhu, Z., 2023. Removal of dioxins from municipal solid waste incineration fly ash by low-temperature thermal treatment: Laboratory simulation of degradation and ash discharge stages. Waste Manag. 168, 45–53. https://doi.org/10.1016/j.wasman.2023.05.044.

Li, X., Sun, Y., Li, W., Nie, Y., Wang, F., Bian, R., Wang, H., Wang, Y., Gong, Z., Lu, J., Gao, W., Lu, C., 2024. Solidification/stabilization pre-treatment coupled with landfill disposal of heavy metals in MSWI fly ash in China: A systematic review. J. of Hazar. Mat. 478, 135479. https://doi.org/10.1016/j.jhazmat.2024.135479.

Liu, Q., Huang, Q., Zhao, Y., Liu, Y., Wang, Q., Khan, M.A., Che, X., Li, X., Bai, Y., Su, X., Lin, L., Zhao, Y., Chen, Y., Wang, J., 2022a. Dissolved organic matter (DOM) was detected in MSWI plant: An investigation of DOM and potential toxic elements variation in the bottom ash and fly ash. Sci. Total Environ. 828, 154339. https://doi.org/10.1016/j.scitotenv.2022.154339.

Liu, J., Wang, Z., Xie, G., Li, Z., Fan, X., Zhang, W., Ren, J., 2022b. Resource utilization of municipal solid waste incineration fly ash-cement and alkali-activated cementitious materials: A review. Sci. Total Environ. 158254. https://doi.org/10.1016/j.scitotenv.2022.158254.

Liu, Y., Molinari, S., Dalconi, M.C., Valentini, L., Ricci, G., Carrer, C., Ferrari, G., Artioli, G., 2023. The leaching behaviors of lead, zinc, and sulfate in pyrite ash contaminated soil: mineralogical assessments and environmental implications. J. Environ. Chem. Eng. 11, 109687. https://doi.org/10.1016/j.jece.2023.109687.

Loginova, E., Proskurnin, M., Brouwers, H.J.H., 2019. Municipal solid waste incineration (MSWI) fly ash composition analysis: A case study of combined chelatant-based washing treatment efficiency. J Environ Manag. 235, 480–488. https://doi.org/10.1016/j.jenvman.2019.01.096.

Matabane, D.L., Godeto, T.W., Mampa, R.M., Ambushe, A.A., 2021. Sequential Extraction and Risk Assessment of Potentially Toxic Elements in River Sediments. Minerals 11, 874. https://doi.org/10.3390/min11080874.

Mazzanti, M., Zoboli, R., 2008. Waste generation, waste disposal and policy effectiveness: Evidence on decoupling from the European Union. Resour. Conserv. Recycl. 52, 1221–1234. https://doi.org/10.1016/j.resconrec.2008.07.003.

Meima, J.A., Comans, R.N.J., 1999. The leaching of trace elements from municipal solid waste incinerator bottom ash at different stages of weathering. Appl. Geochem. 14, 159–171. https://doi.org/10.1016/S0883-2927(98)00047-X.

Meima, J.A., Comans, R.N.J., 1998. Reducing Sb-leaching from municipal solid waste incinerator bottom ash by addition of sorbent minerals. J. Geochem. Explor. 62, 299–304. https://doi.org/10.1016/S0375-6742(97)00044-7.

Natali, C., Bianchini, G., Vittori Antisari, L., 2018. Thermal separation coupled with elemental and isotopic analysis: A method for soil carbon characterization. Catena 164, 150–157. https://doi.org/10.1016/j.catena.2018.02.022.

Nowak, B., Pessl, A., Aschenbrenner, P., Szentannai, P., Mattenberger, H., Rechberger, H., Winter, F., 2010. Heavy metal removal from municipal solid waste fly ash by chlorination and thermal treatment. J. Hazard. Mater. 179, 323–331. https://doi.org/10.1016/j.jhazmat.2010.03.008.

Picó, Y., Barceló, D., 2022. Mass Spectrometry in Food and Environmental Chemistry 99–125. https://doi.org/10.1007/698_2022_907.

Qin, J., Zhang, Y., Yi, Y., 2023. Water washing and acid washing of gasification fly ash from municipal solid waste: Heavy metal behavior and characterization of residues. Environ. Pollut. 320, 121043. https://doi.org/10.1016/j.envpol.2023.121043.

Righi, C., Lancellotti, I., Barbieri, L., Kirkelund, G.M., 2022. Benefits of pre-treating MSWI fly ash before alkali-activation. Sustain. Chem. Pharm. 27, 100671. https://doi.org/10.1016/j.scp.2022.100671.

Test Method SW-846 1313: Liquid-Solid Partitioning as a Function of Extract pH Using a Parallel Batch Extraction Procedure. US EPA, 2017. https://www.epa.gov/sites/default/files/2017-10/documents/method_1313_-_final_8-3-17.pdf.

Tiberg, C., Sjöstedt, C., Fedje, K.K., 2020. Speciation of Cu and Zn in bottom ash from solid waste incineration studied by XAS, XRD, and geochemical modelling. Waste Manag. 119, 389–398. https://doi.org/10.1016/j.wasman.2020.10.023.

Toby, B.H., Von Dreele, R.B., 2013. GSAS-II: the genesis of a modern open-source all purpose crystallography software package. J. Appl. Crystallogr. 46, 544–549. https://doi.org/10.1107/S0021889813003531.

Tong, L., He, J., Wang, F., Wang, Y., Wang, L., Tsang, D., Hu, Q., Hu, B., Tang, Y., 2020. Evaluation of the BCR sequential extraction scheme for trace metal fractionation of

alkaline municipal solid waste incineration fly ash. Chemosphere 249, 126115. https://doi.org/10.1016/j.chemosphere.2020.126115.
Xu, P., Zhao, Q., Qiu, W., Xue, Y., Li, N., 2019. Microstructure and Strength of Alkali-Activated Bricks Containing Municipal Solid Waste Incineration (MSWI) Fly Ash Developed as Construction Materials. Sustainability. 11, 1283. https://doi.org/10.3390/su11051283.
Xue, Y., Liu, X., 2021. Detoxification, solidification and recycling of municipal solid waste incineration fly ash: A review. Chem. Eng. J. 420, 130349. https://doi.org/10.1016/j.cej.2021.130349.
Wagner, T., Magill, C.R., Herrle, J.O. Carbon isotopes. In: Encyclopedia of Geochemistry: A Comprehensive Reference Source on the Chemistry of the Earth (Ed. W.M. White), 2018, 194–204. Springer, Cham. DOI: 10.1007/978-3-319-39312-4_176.
Wang, H., Lv, Z., Wang, B., Wang, Y., Sun, Y., Tsang, Y.F., Zhao, J., Zhan, M., 2019. Effective stabilization of antimony in Waste-to-Energy fly ash with recycled laboratory iron–rich residuals. J. Clean. Prod. 230, 685–693. https://doi.org/10.1016/j.jclepro.2019.05.128.
Wang, H., Zhao, B., Zhu, F., Chen, Q., Zhou, T., Wang, Y., 2023. Study on the reduction of chlorine and heavy metals in municipal solid waste incineration fly ash by organic acid and microwave treatment and the variation of environmental risk of heavy metals. Sci. Total Environ. 870, 161929. https://doi.org/10.1016/j.scitotenv.2023.161929.
Watari, T., Nansai, K., Nakajima, K., 2021. Major metals demand, supply, and environmental impacts to 2100: A critical review. Resour. Conserv. Recycl. 164, 105107. https://doi.org/10.1016/j.resconrec.2020.105107.
Weibel, G., Eggenberger, U., Kulik, D.A., Hummel, W., Schlumberger, S., Klink, W., Fisch, M., Mäder, U., 2018. Extraction of heavy metals from MSWI fly ash using hydrochloric acid and sodium chloride solution. Waste Manag. 76, 457–471. https://doi.org/10.1016/j.wasman.2018.03.022.
Wolffers, M., Eggenberger, U., Schlumberger, S., Churakov, S.V., 2021. Characterization of MSWI fly ashes along the flue gas cooling path and implications on heavy metal recovery through acid leaching. Waste Manag. 134, 231–240. https://doi.org/10.1016/j.wasman.2021.08.022.
Zhang, S., Chen, Z., Lin, X., Wang, F., Yan, J., 2020. Kinetics and fusion characteristics of municipal solid waste incineration fly ash during thermal treatment. Fuel 279, 118410. https://doi.org/10.1016/j.fuel.2020.118410.
Zhang, Y., Jiang, J., Chen, M., 2008. MINTEQ modeling for evaluating the leaching behavior of heavy metals in MSWI fly ash. J. Environ. Sciences 20, 1398–1402. https://doi.org/10.1016/S1001-0742(08)62239-1.
Zhang, Y., Wang, L., Chen, L., Ma, B., Zhang, Y., Ni, W., Tsang, D.C.W., 2021. Treatment of municipal solid waste incineration fly ash: State-of-the-art technologies and future perspectives. J. of Hazar. Mat. 411, 125132. https://doi.org/10.1016/j.jhazmat.2021.125132.
Zhao, K., Hu, Y., Tian, Y., Chen, D., Feng, Y., 2020. Chlorine removal from MSWI fly ash by thermal treatment: Effects of iron/aluminum additives. J. Environ. Sciences 88, 112–121. https://doi.org/10.1016/j.jes.2019.08.006.